RSC Advances

PAPER

View Article Online
View Journal | View Issue

Cite this: *RSC Adv.*, 2017, **7**, 16602

Bi_2O_3 modification of HZSM-5 for methanol-to-propylene conversion: evidence of olefin-based cycle

Hairong Zhang,[a] Zhangxuan Ning,[a] Hongyan Liu,*[a] Jianpeng Shang,[a] Shenghua Han,[a] Dingding Jiang,[a] Yu Jiang[b] and Yong Guo*[a]

Received 6th December 2016
Accepted 3rd March 2017

DOI: 10.1039/c6ra27849c

rsc.li/rsc-advances

Bi_2O_3-modified HZSM-5 catalysts were prepared *via* a traditional wetness impregnation approach, and used for the methanol-to-propylene conversion reaction. The selectivity for propylene increases significantly with bismuth loading, while that for ethylene shows the opposite trend. However, the Bi_2O_3/HZSM-5 catalysts have significantly lower capacities for methanol conversion than the parent HZSM-5. The underlying causes are the reduced acid site strength, narrower pore openings, and reduced pore width in Bi_2O_3/HZSM-5. This work provides insights into the olefin-based cycle operation for methanol-to-olefin reactions using modified HZSM-5 catalysts.

Introduction

Because methanol can be produced from natural gas, coal, biomass, or CO_2 hydrogenation,[1] the methanol-to-propylene (MTP) process is an alternative route to produce propylene with high yield and high propylene/ethylene ratio (P/E). This process was first developed by the Lurgi company based on a fixed bed reactor with a high-silica nanosized HZSM-5 zeolite catalyst, and the process was commercialised in China in 2010.[2] During the past four decades, many attempts have been made to selectively produce propylene from methanol,[3] not only on medium-pore zeolites (ZSM-5, EU-2) but also on small-pore (HFU-1, SAPO-34, Sigma-1, and ZSM-58 (ref. 4)) and large-pore zeolites (modified Y zeolites, Mn/ZSM-12, Ba/dealuminated mordenite, and CON[5]). There are four general strategies to improve propylene selectivity in the methanol-to-olefin (MTO) reaction:

(1) Reducing the Brønsted acidity (in terms of both site density and strength) of zeolite catalysts[6,7] in order to limit/inhibit the side reactions. The approaches include: adjusting the Si/Al ratio of the zeolite,[8–10] post-synthesis modification,[11–16] and isomorphous substitution of heteroatoms for zeolite.[5,17–21]

(2) Modifying the porosity of the zeolite and thereby influencing the transition state shape selectivity, such as by using zeolites with different topologies[22–30] or tailoring their pore size by post-synthesis modification.[31–33] Moreover, a shorter diffusion length in zeolites enhances the molecular diffusion,[34] which may dramatically influence the product shape selectivity.[27] This could be achieved *via* either reducing the particle size[35–37] or introducing an additional mesoporous transport network.[20,21,23,38–50]

(3) Modifying the reaction conditions, such as diluting methanol with an inert gas or co-feeding water,[3,13,51] and changing the temperature. It is generally known that the addition of water stabilises of the catalyst during the MTO reaction, and that the product distribution may change according to the partial pressure of methanol.[3,4,28] Reducing the partial pressure and weight hourly space velocity (WHSV) of methanol could possibly suppress the influence of hydrogen transfer reactions over H–T zeolite.[52] Water competes with light olefins for the Brønsted and Lewis acid sites, and accelerates the desorption of the olefins.[3,4] Therefore, the adsorption of water on these acid centres reduces their strength and concentration, as well as their probability of interaction with hydrocarbons. As a consequence, the initial conversion of light olefins (mainly propylene) into oligomers, aromatics, and coke is lowered.[3] However, while a high P/E ratio can be achieved with a low methanol partial pressure, a very low value of the latter is not economical for practical operations.[37] (4) Changing the reactor configuration.

It is known that in the reactions of toluene disproportionation, methylation of toluene, and xylene isomerisation, post-synthesis modification of HZSM-5 with oxides not only decreased the Brønsted acidity (density and strength) of the zeolite catalyst, but also narrowed/blocked the pore openings and reduced the pore size.[53] This may affect the transition state shape selectivity and enhance the para-selectivity for toluene disproportionation. In the case of MTO reaction, it is well accepted that the zeolite performance is controlled by its framework structure, pore architecture, and acidity. The product distribution in methanol to hydrocarbon conversion over ZSM-5 can be rationalised in terms of the relative propagation rates of the aromatic- and olefin-based cycles.[50] If we

[a]*College of Chemistry and Chemical Engineering, Institute of Applied Chemistry, Shanxi Datong University, Datong 037009, P. R. China. E-mail: liuhongyan@tyut.edu.cn; liuhongyan9629@163.com; ybsy_guo@163.com*

[b]*Datong Coal Mine Group Co., LTD, Datong 037003, P. R. China*

separate these two cycles by sterically suppressing the formation of the larger aromatic molecules and only allowing product formation *via* the C_{3+} alkenes, ethylene formation might be avoided in the MTP application.[23] However, few experimental studies have been conducted using such steric constraints to suppress the aromatic-based cycles.[25,51,54]

In this study, bismuth oxide-modified HZSM-5 catalysts were prepared by a wetness impregnation method. The catalysts were characterised by X-ray powder diffraction (XRD), Brunauer–Emmett–Teller (BET) adsorption, and NH_3 temperature programmed desorption (TPD) analyses. Their catalytic activities for MTP conversion were tested. Our main goal was to understand the influence of the acidic properties and microporous structure of HZSM-5 on its catalytic performance. We are especially interested in their effects as well as those of the methanol WHSV on the dual cycles.

Experimental

Catalyst preparation

The ZSM-5 zeolite was hydrothermally synthesised according to our previous work.[55] The parent HZSM-5 was prepared by ion exchange of ZSM-5 three times in 1 M NH_4NO_3 solution at 90 °C for 4 h each time. After filtration, the residue was dried at 100 °C for 12 h, and further calcined at 550 °C in air for 6 h.

The HZSM-5 catalyst was modified by Bi_2O_3 using a wetness impregnation method. The bare HZSM-5 was mixed with a solution containing the desired amount of bismuth nitrate in deionised water. Thereafter, the solution was transferred into a vacuum evaporator to eliminate the water. The residue was dried at 100 °C for 12 h, and further calcined at 550 °C in air for 6 h. The catalysts with 3 or 5 wt% Bi_2O_3 in HZSM-5 were denoted a and b, respectively.

Catalyst characterisation

The XRD patterns were acquired on a Shimadzu XRD-6000 diffractometer operated at 40 kV and 40 mA with Cu Kα irradiation and nickel filter (λ = 0.15406 nm). The diffraction patterns were recorded in the angle range of 2θ = 5–35° with a scan speed of 8.0° min^{-1}. The specific surface areas, pore size distributions, and total pore volumes of the catalysts were obtained *via* N_2 adsorption/desorption at −196 °C using a Micromeritics ASAP 2010 apparatus, after first outgassing the sample at 300 °C for 4 h under vacuum. Specific surface areas were calculated according to the BET method. NH_3-TPD analysis was performed in a quartz fixed-bed micro-reactor equipped with a thermal conductivity detector. Prior to the experiment, 100 mg of the catalyst was pre-treated in a He stream (99.99%, 20 mL min^{-1}) at 400 °C for 0.5 h. After cooling down to 100 °C, the catalyst was exposed to a flow of 20 vol% NH_3/N_2 mixture (30 mL min^{-1}) for 30 min, and then treated in an N_2 flow for 40 min in order to remove any physically adsorbed molecules. Finally, the desorption experiment was carried out in an N_2 flow (99.99%, 20 mL min^{-1}) from 100–600 °C at a heating rate of 10 °C min^{-1}.

Catalytic tests

The MTP reaction was carried out at atmospheric pressure in a fixed-bed stainless steel reactor (i.d.: 15 mm, length: 550 mm). The catalyst powder was compressed to form wafers, then crushed and sieved to obtain 40–60 mesh particles. In all the experiments, 0.5 g of the catalyst was placed in the middle of the reactor and activated *in situ* at 550 °C for 3 h under an N_2 flow of 30 mL min^{-1}. The total products were analysed online with a gas chromatograph (GC-950) equipped with a flame ionisation detector and an HP-Plot Q capillary column (30 m, 0.53 mm i.d., stationary phase thickness 40 μm). Both methanol and dimethylether(DME) were regarded as reactants in the calculations.

Results and discussion

Effect of Bi_2O_3 on the structure and acidity of HZSM-5

In Fig. 1, the similar XRD patterns of all zeolite samples indicate that the framework of HZSM-5 was preserved after the modification. However, the relative intensities changed slightly, meaning that the crystallinity of the catalysts is influenced by the amount of Bi_2O_3 used for modification. Compared to the HZSM-5 sample and using the intensities of the typical MFI peaks of 501, 051, 151, 303, and 133,[56] the relative crystallinities of a and b were estimated as 89.8% and 78.1%, respectively. The crystalline phases of Bi_2O_3 were not detected in the modified zeolites with up to 5 wt% Bi_2O_3. This suggests that some of the Bi_2O_3 was dispersed on the external surface of zeolite in the form of nanosized crystal particles,[57,58] which is one reason for the reduced crystallinity after the modification. Moreover, compared with HZSM-5, the intensities of XRD peaks with 2θ < 10° in a and b decreased evidently. This observation implies that Bi_2O_3 entered the zeolite channels, since the low-angle XRD intensities for ZSM-5 are known to be sensitive to the presence of any species inside the channels.[56,59–62]

We made two interesting discoveries. First, the main XRD peak shifts to a lower angle upon the incorporation of more bismuth. Most modified HZSM-5 zeolite catalysts[13,14,56,63–70] and ZSM-5 zeolite with increased Si/Al ratio[8,30,71,72] display this

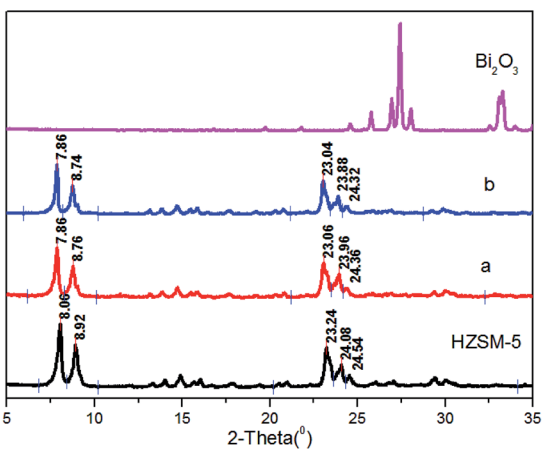

Fig. 1 XRD patterns for the samples. Bottom to top: HZSM-5, (a) 3 wt% Bi_2O_3/HZSM-5, (b) 5 wt% Bi_2O_3/HZSM-5, and Bi_2O_3.

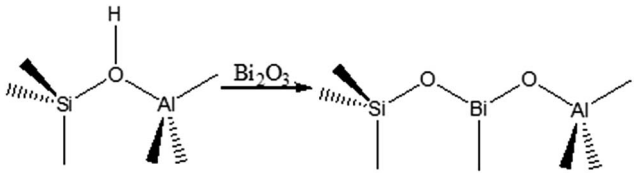

Fig. 2 Proposed interactions between Bi_2O_3 and Brønsted acidity.

behaviour. Second, the framework tetrahedral Al is preserved and the framework Al shifts slightly downfield (in ^{27}Al MAS NMR spectra) compared to modified HZSM-5 zeolite. The ^{27}Al MAS NMR spectra of HZSM-5 is known to contain two signals: an intense peak centred at 55 ppm (the framework tetrahedral Al), and a weak signal centred at 0 ppm (extra-framework Al).[32,37,73] In phosphorous-modified ZSM-5 zeolite,[64] the NMR spectrum shows that all the Al exists as framework tetrahedral Al, and the peak corresponding to framework Al shifts slightly downfield (from 53.3 to 56.5 ppm) after phosphate treatment. In Mo-modified ZSM-5 zeolite,[70] the peak corresponding to framework tetrahedral Al was shifted to higher fields by −2.5 ppm. Based on these reports, we speculate that the introduced Bi_2O_3 not only reduced the Brønsted acid sites in ZSM-5 zeolite, but also formed defects in the ZSM-5 structure (Fig. 2). These structural defects in the HZSM-5 structure are another reason for the lower crystallinity in the modified zeolites.

Table 1 shows the BET specific surface area (t-micro-pore and t-meso-pore), pore volume (t-micro-pore), and pore size of the catalysts calculated from the N_2 adsorption/desorption isotherms. All the parameters decreased in value after 3 wt% Bi_2O_3 loading: the total pore volume shrunk by 22.5%, the BET surface area and microporous volume decreased respectively by 14.9% and 13.9%, and the pore size decreased by 22.9% compared to the parent HZSM-5. These changes further imply that some of the bismuth was dispersed on the surface and the rest entered the channels of HZSM-5. Between 3 wt% and 5 wt% Bi_2O_3 loading, the structural parameters only changed slightly, indicating that the deposition of Bi_2O_3 partially blocked the pore openings and hence restricted further penetration of Bi_2O_3 into the pores. In other words, a small amount of Bi_2O_3 penetrated the pores of HZSM-5, while a larger fraction of Bi_2O_3 was located on the external surface of the HZSM-5 zeolite crystals. This resulted in the narrowed pore openings and reduced apparent pore size for the HZSM-5 zeolite channels.

Table 1 Textural and structural parameters of HZSM-5 catalysts before and after bismuth modification

	Specific surface area $m^2\ g^{-1}$			Pore volume $cm^{-3}\ g^{-1}$		Pore size nm
Catalysts	S_{BET}	S_{mic}	S_{mes}	Total	V_{mic}	BJH
HZSM-5	388	356.0	32.0	0.2422	0.1774	2.17
a	330	308.0	22.0	0.1878	0.1527	1.67
b	323	302.0	21.0	0.1804	0.1456	1.67

Acidity is one of the most important characteristics of aluminosilicate zeolites, because the amount and strength of the acid sites are key for the catalytic performance. The NH_3-TPD measurements were used to determine these characteristics. In Fig. 3, all three catalysts showed two distinct desorption peaks in the TPD profiles, in accordance with the reported data for MFI materials.[21] In general, the desorption temperature represents the strength of acid sites: the peak at the lower (higher) temperature is associated with the weak (strong) acid sites. After 3% Bi_2O_3 loading, the number of strong acid sites decreased sharply and the ammonium desorption temperature was slightly lower than that of HZSM-5, while those of the weak acid sites showed the opposite trend. When the Bi_2O_3 loading was increased to 5%, the acidity trend remained similar to that for a, hence the amount of acid sites remained approximately the same. We conclude that the concentration and strength of the strong acid sites in the bismuth-containing HZSM-5 catalysts decrease with increasing Bi_2O_3 content, while those of weak acid sites increase, in agreement with other modified HZSM-5 catalysts.[11]

Effect of Bi_2O_3 on catalytic performance in the MTP reaction

Catalyst conversion capacities. The conversion capacities of the catalysts for MTP reaction were evaluated in a continuous flow fixed bed reactor under atmospheric pressure at 470 °C, using a mixture of 50 mol% methanol in water with methanol WHSV from 1 to 21 h^{-1}. The catalyst conversion capacities were estimated by using the methanol WHSV for complete methanol conversion at a certain reaction time. In the results (Fig. 4A), with WHSV from 1 to 2 h^{-1} at early time-on-stream, the bismuth-containing HZSM-5 catalysts displayed higher methanol conversion than the parent HZSM-5. During the MTO/MTP processes, methanol molecules diffuse into the zeolite pores and react at the active sites to produce light olefins (*e.g.*, ethylene, propylene, and butylenes). Then the rapid secondary reactions could form paraffins, aromatics, and higher olefins by hydrogen transfer, alkylation, and polycondensation.[3] The

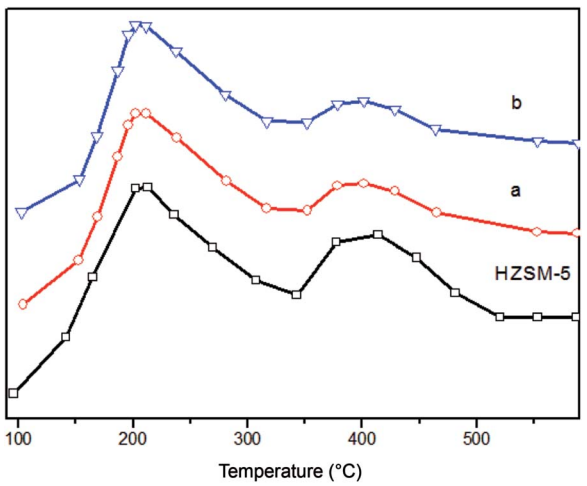

Fig. 3 NH_3-TPD profiles of the samples: HZSM-5, 3 wt% Bi_2O_3/HZSM-5 (a), and 5 wt% Bi_2O_3/HZSM-5 (b).

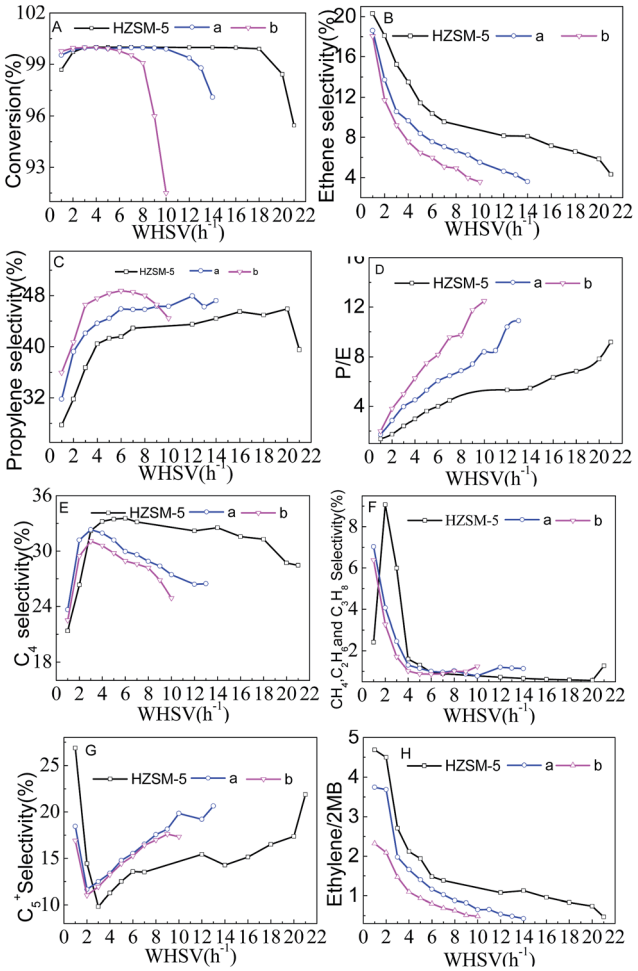

Fig. 4 Methanol conversion and product selectivity *vs.* WHSV using different zeolite catalysts. Reaction conditions: P = 0.1 MPa, and n(MeOH)/n(H_2O) = 1/1.

general consensus is that the intermediate in the dehydration reaction of methanol to dimethyl ether over solid acid catalysts is the surface methoxy group [$SiO(CH_3)Al$]. The highly reactive surface methoxy species can contribute to the methylation of alkenes, alkanes, and aromatics, leading to the formation of a hydrocarbon pool to start the MTO/MTG process.[74,75] The narrowed pore openings of ZSM-5 in a and b limit the diffusion of reactants and products within the catalysts. Therefore, the hydrocarbon pool species easily accumulate within the pores, thereby enhancing the autocatalytic effect. From Fig. 4F and E, a and b produced less C_5^+ hydrocarbons than the parent HZSM-5, together with very low yields of C_1–C_4 saturated hydrocarbons. The results obviously show that the bismuth-containing HZSM-5 catalysts could reduce the catalyst induction period and increase the rate of methanol conversion (Fig. 4A).

With further increase in the methanol WHSV, the catalysts exhibited nearly 100% methanol conversion. In the case of HZSM-5, the transformation of methanol remained approximately 100% at WHSV = 18 h^{-1} and then declined to 95.5% at 21 h^{-1}. However, the methanol conversion for a remained at approximately 100% at WHSV = 12 and then declined to 96.6% at 14 h^{-1}. Similarly, the value for b was about 100% and 91.5% at WHSV = 6 and 10 h^{-1}, respectively. The conversion capacities of bismuth-containing HZSM-5 catalysts were noticeably lower. A similar phenomenon was described for the HZSM-5 zeolite co-modified with P and Mn.[64] The observations in this study can be explained by the reduced concentration and strength of the strong acid sites, narrowed pore openings, and reduced apparent pore size of the channels of the bismuth-containing HZSM-5 catalysts (a and b). It is known that the density and strength of acid sites have profound effects on the activity and lifetime of zeolite catalysts.[76] Since the diffusion limitation increases with the Bi_2O_3 loading, the lower conversion capacities after the bismuth loading may also be partly due to the higher diffusional resistance that reduces the overall reaction rates.

Product selectivity. The selectivities for different hydrocarbons with varying methanol WHSV are shown in Fig. 4B–G. It can be seen from Fig. 4B that the ethylene selectivity decreased with increasing methanol WHSV, in close agreement with the results by Dessau[77] (which indicate that ethylene was only obtained at low WHSV, *i.e.*, long contact times). At identical reaction conditions, a and b displayed lower ethylene selectivity than the parent HZSM-5. Especially, the ethylene selectivity decreases with decreasing pore volume and pore size of the catalyst.

From Fig. 4C and E, the selectivities for propylene and butylenes first increased and then decreased with increasing methanol WHSV, whereas the opposite trend (Fig. 4F and G) was observed for lower alkanes (C_1–C_4) and liquid heavy hydrocarbons (C_5^+ hydrocarbons or aromatics). The selectivity toward propylene appears to be ordered as b > a > unmodified HZSM-5. This may be due to the strong correlation among the pore volume, pore size, and number of acid sites. Increased Bi_2O_3 loading reduces the number of acidic sites, which can successfully suppress the hydride transfer and propylene oligomerisation reactions.

The ratio between the propylene and ethylene selectivities (P/E ratio) as a function of methanol WHSV is shown in Fig. 4D. The P/E ratio was enhanced with increasing WHSV, albeit at the expense of the methanol conversion, in agreement with the report by Losch *et al.*[7] Under identical reaction conditions, the P/E ratios for a and b are higher than that of the parent HZSM-5. Especially, this ratio is increased while the pore volume and pore size of the catalyst are decreased. The research of Teketel *et al.* shows that even subtle changes in the pore size may dramatically influence the product shape selectivity.[27]

It is generally accepted that two catalytic cycles occur simultaneously during the MTH (methanol to hydrocarbon) reaction over HZSM-5 zeolite: the aromatic-based cycle (ethene formation from the lower methylbenzenes followed by remethylation), and the olefin-based cycle (a methylation/cracking cycle involving only the C_{3+} alkenes).[78] Narrowing the pore openings and reducing the apparent pore size of the HZSM-5 channels are likely to suppress the aromatic-based cycle that requires more space, and favour the alkene cracking and methylation.[54] The ratio of ethene to (2-methylbutane + 2-methyl-2-butene) yields (ethene/2 MB) can be used to describe

the relative propagation of the aromatic- and olefin-based cycles in MTH catalysed by HZSM-5, where a high (low) ethene/2 MB ratio indicates increased propagation of the aromatic-based (olefin-based) cycle.[50] From Fig. 4H, the ethene/2 MB ratio became lower with increasing methanol WHSV. Under identical reaction conditions, the ratios for catalysts a and b are lower than that for the parent HZSM-5. Especially, this ratio decreases with decreasing pore volume and pore size of the catalysts. Apparently, increasing the methanol WHSV or Bi_2O_3 loading can facilitate the propagation of the olefin-based cycle, thereby improving the propylene selectivity and reduce the ethylene selectivity. Hence, the P/E ratio is improved.

Conclusions

Bi_2O_3-modified HZSM-5 catalysts showed substantial propylene selectivity and improved P/E ratios in the conversion of methanol to propylene, compared with the parent HZSM-5 zeolite catalyst. The enhanced catalytic performance can be attributed to the narrowing of the pore openings, reduced the apparent pore size of the HZSM-5 zeolite channels, together with the lowered Brønsted acidity. Increasing the methanol WHSV also enhanced the propylene selectivity and P/E ratio, although at the expense of methanol conversion. These results contribute to the fundamental understanding of selectivity control in the MTP reaction. The approach discussed here can also be used for the rational design of new catalysts for this process. In fact, we have designed a high effective MTP catalyst by a direct synthetic method.

Acknowledgements

This work has been supported by the National Nature Science Foundation of China (No. 51303098, 21477069, and 21506120), Datong Science and Technology Public Relations Project (2015021), and the Doctoral Science Foundation of ShanXiDa-Tong University (No. QD201049). We also thank Dian-Hua Song, Yao-Ya Luo, Yi-Bo Gong, Jin-Yi Cao, and Bing-Xi Wang for their assistance with the reaction experiments.

Notes and references

1 O. Martin, A. J. Martín, C. Mondelli, S. Mitchell, T. F. Segawa, R. Hauert, C. Drouilly, D. Curulla-Ferré and J. Pérez-Ramírez, *Angew. Chem.*, 2016, **55**, 6261–6265.
2 Agudamu, Y. Sun and F. Zhang, Coal Chemistry Industry, 2013, 58–60.
3 M. Stöcker, *Microporous Mesoporous Mater.*, 1999, **29**, 3–48.
4 Y. Kumita, J. Gascon, E. Stavitski, J. A. Moulijn and F. Kapteijn, *Appl. Catal., A*, 2011, **391**, 234–243.
5 M. Yoshioka, T. Yokoi and T. Tatsumi, *ACS Catal.*, 2015, **5**, 4268–4275.
6 C. D. Chang, C. T.-W. Chu and A. R. F. Socha, *J. Catal.*, 1984, **86**, 289–296.
7 P. Losch, M. Boltz, B. Louis, S. Chavan and U. Olsbye, *C. R. Chim.*, 2015, **18**, 330–335.
8 R. Wei, C. Li, C. Yang and H. Shan, *J. Nat. Gas Chem.*, 2011, **20**, 261–265.
9 Y. Kim, J. C. Kim, C. Jo, T. W. Kim, C. U. Kim, S. Y. Jeong and H. J. Chae, *Microporous Mesoporous Mater.*, 2016, **222**, 1–8.
10 L. Zhang, H. Wang, G. Liu, K. Gao and J. Wu, *J. Mol. Catal. A: Chem.*, 2015, **411**, 311–316.
11 J. Liu, C. Zhang, Z. Shen, W. Hua, Y. Tang, W. Shen, Y. Yue and H. Xu, *Catal. Commun.*, 2009, **10**, 1506–1509.
12 D. V. Vu, Y. Hirota, N. Nishiyama, Y. Egashira and K. Ueyama, *J. Jpn. Pet. Inst.*, 2010, **53**, 232–238.
13 J. M. Man, Q. D. Zhang, H. J. Xie, J. X. Pan, Y. S. Tan and Y. Z. Han, *J. Fuel Chem. Technol.*, 2011, **39**, 42–46.
14 X. Wang, W. Dai, G. Wu, L. Li, N. Guan and M. Hunger, *Microporous Mesoporous Mater.*, 2011, **151**, 99–106.
15 S. Hajimirzaee, M. Ainte, B. Soltani, R. M. Behbahani, G. A. Leeke and J. Wood, *Chem. Eng. Res. Des.*, 2015, **93**, 541–553.
16 M. Rostamizadeh and A. Taeb, *J. Ind. Eng. Chem.*, 2015, **27**, 297–306.
17 Y. Yang, C. Sun, J. Du, Y. Yue, W. Hua, C. Zhang, W. Shen and H. Xu, *Catal. Commun.*, 2012, **24**, 44–47.
18 Y. Jin, S. Asaoka, S. Zhang, P. Li and S. Zhao, *Fuel Process. Technol.*, 2013, **115**, 34–41.
19 H. R. Zhang, H. Y. Liu, Y. Jiang, X. H. Chang, K. Yuan, B. Wang, Y. Guo and S. M. Meng, *Adv. Mater. Res.*, 2013, **834–836**, 476–480.
20 F. Yaripour, Z. Shariatinia, S. Sahebdelfar and A. Irandoukht, *Microporous Mesoporous Mater.*, 2015, **203**, 41–53.
21 Z. Hu, H. Zhang, L. Wang, H. Zhang, Y. Zhang, H. Xu, W. Shen and Y. Tang, *Catal. Sci. Technol.*, 2014, **4**, 2891–2895.
22 M. Bjørgen, U. Olsbye, D. Petersen and S. Kolboe, *J. Catal.*, 2004, **221**, 1–10.
23 S. Svelle, F. Joensen, J. Nerlov, U. Olsbye, K. Lillerud, A. S. Kolboe and M. Bjørgen, *J. Am. Chem. Soc.*, 2006, **128**, 14770–14771.
24 Q. Zhu, J. N. Kondo, T. Tatsumi, S. Inagaki, R. Ohnuma, Y. Kubota, Y. Shimodaira, H. Kobayashi and K. Domen, *J. Phys. Chem. C*, 2007, **111**, 5409–5415.
25 Z. M. Cui, Q. Liu, W. G. Song and L. J. Wan, *Angew. Chem., Int. Ed.*, 2006, **45**, 6512–6515.
26 S. Hu, Y. Gong, Q. Xu, X. Liu, Q. Zhang, L. Zhang and T. Dou, *Catal. Commun.*, 2012, **28**, 95–99.
27 S. Teketel, W. Skistad, S. Benard, U. Olsbye, K. P. Lillerud, P. Beato and S. Svelle, *ACS Catal.*, 2012, **2**, 26–37.
28 F. F. Wei, Z. M. Cui, X. J. Meng, C. Y. Cao, F. S. Xiao and W. G. Song, *ACS Catal.*, 2014, **4**, 529–534.
29 J. Li, Y. Wei, J. Chen, S. Xu, P. Tian, X. Yang, B. Li, J. Wang and Z. Liu, *ACS Catal.*, 2015, **5**, 661–665.
30 S. Papari, A. Mohammadrezaei, M. Asadi, R. Golhosseini and A. Naderifar, *Catal. Commun.*, 2011, **16**, 150–154.
31 A. M. Al-Jarallah, U. A. El-Nafaty and M. M. Abdillahi, *Appl. Catal., A*, 1997, **154**, 117–127.
32 S. Hu, J. Shan, Q. Zhang, Y. Wang, Y. Liu, Y. Gong, Z. Wu and T. Dou, *Appl. Catal., A*, 2012, **445–446**, 215–220.
33 M. Firoozi, M. Baghalha and M. Asadi, *Catal. Commun.*, 2009, **10**, 1582–1585.

34 H.-G. Jang, H.-K. Min, J. K. Lee, S. B. Hong and G. Seo, *Appl. Catal., A*, 2012, **437–438**, 120–130.
35 A. K. Jamil, O. Muraza, M. Yoshioka, A. M. Alamer, Z. H. Yamani and T. Yokoi, *Ind. Eng. Chem. Res.*, 2014, **53**, 19498–19505.
36 F. C. Patcas, *J. Catal.*, 2005, **231**, 194–200.
37 C. Mei, P. Wen, Z. Liu, H. Liu, Y. Wang, W. Yang, Z. Xie, W. Hua and Z. Gao, *J. Catal.*, 2008, **258**, 243–249.
38 S. Ivanova, C. Lebrun, E. Vanhaecke, C. Pham-Huu and B. Louis, *J. Catal.*, 2009, **265**, 1–7.
39 Y. Jiao, C. Jiang, Z. Yang and J. Zhang, *Microporous Mesoporous Mater.*, 2012, **162**, 152–158.
40 Y. Jiao, C. Jiang, Z. Yang, J. Liu and J. Zhang, *Microporous Mesoporous Mater.*, 2013, **181**, 201–207.
41 Q. Zhang, S. Hu, L. Zhang, Z. Wu, Y. Gong and T. Dou, *Green Chem.*, 2014, **16**, 77–81.
42 F. Schmidt, M. R. Lohe, B. Büchner, F. Giordanino, F. Bonino and S. Kaskel, *Microporous Mesoporous Mater.*, 2013, **165**, 148–157.
43 J. Ahmadpour and M. Taghizadeh, *J. Nat. Gas Sci. Eng.*, 2015, **23**, 184–194.
44 M. Wen, X. Wang, L. Han, J. Ding, Y. Sun, Y. Liu and Y. Lu, *Microporous Mesoporous Mater.*, 2015, **206**, 8–16.
45 J. Ding, L. Han, M. Wen, G. Zhao, Y. Liu and Y. Lu, *Catal. Commun.*, 2015, **72**, 156–160.
46 Y. Jiao, X. Yang, C. Jiang, C. Tian, Z. Yang and J. Zhang, *J. Catal.*, 2015, **332**, 70–76.
47 J. Ahmadpour and M. Taghizadeh, *C. R. Chim.*, 2015, **18**, 834–847.
48 X. Zhu, J. P. Hofmann, B. Mezari, N. Kosinov, L. Wu, Q. Qian, B. M. Weckhuysen, S. Asahina, J. Ruizmartínez and E. J. M. Hensen, *ACS Catal.*, 2016, **6**, 2163–2177.
49 M. Wen, J. Ding, C. Wang, Y. Li, G. Zhao, Y. Liu and Y. Lu, *Microporous Mesoporous Mater.*, 2016, **221**, 187–196.
50 S. Ilias, R. Khare, A. Malek and A. Bhan, *J. Catal.*, 2013, **303**, 135–140.
51 R. Y. Brogaard, R. Henry, Y. Schuurman, A. J. Medford, P. G. Moses, P. Beato, S. Svelle, J. K. Nørskov and U. Olsbye, *J. Catal.*, 2014, **314**, 159–169.
52 G. F. Froment, W. J. H. Dehertog and A. J. Marchi, *Catalysis*, 1992, **9**, 1–64.
53 S. Zheng, A. Jentys and J. A. Lercher, *J. Catal.*, 2003, **219**, 310–319.
54 S. Teketel, U. Olsbye, K. P. Lillerud, P. Beato and S. Svelle, *Microporous Mesoporous Mater.*, 2010, **136**, 33–41.
55 H. Zhang, Q. Zhang, Y. Li, P. Zhang, R. Pan, X. Li and T. Du, *J. Fuel Chem. Technol.*, 2010, **38**, 319–323.
56 D. Dumitriu, R. Bârjega, L. Frunza, D. Macovei, T. Hu, Y. Xie, V. I. Pârvulescu and S. Kaliaguine, *J. Catal.*, 2003, **219**, 337–351.
57 Q. Wang, J. Hui, L. Yang, H. Huang, Y. Cai, S. Yin and Y. Ding, *Appl. Surf. Sci.*, 2014, **289**, 224–229.
58 J. K. Reddy, K. Lalitha, V. Durga Kumari and M. Subrahmanyam, *Catal. Lett.*, 2007, **121**, 131–136.
59 B. Li, S. Li, N. Li, H. Chen, W. Zhang, X. Bao and B. Lin, *Microporous Mesoporous Mater.*, 2006, **88**, 244–253.
60 A. Araya and B. M. Lowe, *Zeolites*, 1986, **6**, 111–118.
61 H. Kosslick, V. A. Tuan, B. Parlitz, R. Fricke, C. Peuker and W. Storek, *J. Chem. Soc., Faraday Trans.*, 1993, **89**, 1131–1138.
62 B. F. Mentzen, M. Sacerdote-Peronnet, J. F. Bérar and F. Lefebvre, *Zeolites*, 1993, **13**, 485–492.
63 T.-S. Zhao, T. Takemoto and N. Tsubaki, *Catal. Commun.*, 2006, **7**, 647–650.
64 H. L. Janardhan, G. V. Shanbhag and A. B. Halgeri, *Appl. Catal., A*, 2014, **471**, 12–18.
65 N. Hadi, A. Niaei, S. R. Nabavi, M. Navaei Shirazi and R. Alizadeh, *J. Ind. Eng. Chem.*, 2015, **29**, 52–62.
66 N. Hadi, A. Niaei, S. R. Nabavi, R. Alizadeh, M. N. Shirazi and B. Izadkhah, *J. Taiwan Inst. Chem. Eng.*, 2016, **59**, 173–185.
67 N. A. S. Amin and D. D. Anggoro, *J. Nat. Gas Chem.*, 2003, **12**, 123–134.
68 D. Goto, Y. Harada, Y. Furumoto, A. Takahashi, T. Fujitani, Y. Oumi, M. Sadakane and T. Sano, *Appl. Catal., A*, 2010, **383**, 89–95.
69 N. Xue, L. Nie, D. Fang, X. Guo, J. Shen, W. Ding and Y. Chen, *Appl. Catal., A*, 2009, **352**, 87–94.
70 J. Tessonnier, B. Louis, S. Walspurger, J. Sommer, A. M. Ledoux and C. Phamhuu, *J. Phys. Chem. B*, 2006, **110**, 10390–10395.
71 A. S. Al-Dughaither and H. de Lasa, *Ind. Eng. Chem. Res.*, 2014, **53**, 15303–15316.
72 T. Armaroli, L. J. Simon, M. Digne, T. Montanari, M. Bevilacqua, V. Valtchev, J. Patarin and G. Busca, *Appl. Catal., A*, 2006, **306**, 78–84.
73 S. M. Campbell, D. M. Bibby, J. M. Coddington, R. F. Howe and R. H. Meinhold, *J. Catal.*, 1996, **161**, 338–349.
74 W. Wang, A. Buchholz, A. Michael Seiler and M. Hunger, *J. Am. Chem. Soc.*, 2003, **125**, 15260–15267.
75 X. Sun, S. Mueller, H. Shi, G. L. Haller, M. Sanchez-Sanchez, A. C. V. Veen and J. A. Lercher, *J. Catal.*, 2014, **314**, 21–31.
76 J. Kim, M. Choi and R. Ryoo, *J. Catal.*, 2010, **269**, 219–228.
77 R. M. Dessau, *J. Catal.*, 1986, **99**, 111–116.
78 S. Svelle, F. Joensen, J. Nerlov, U. Olsbye, K.-P. Lillerud, S. Kolboe and M. Bjørgen, *J. Am. Chem. Soc.*, 2006, **128**, 14770–14771.